Effects of Pressure and the Addition of a Rejected Material from Municipal Waste Composting on the Pyrolysis of Two-Phase Olive Mill Waste

Joan J. Manyà,*[,†] Darío Alvira,[‡] Manuel Azuara,[§] Diana Bernin,[∥] and Niklas Hedin[∥]

[†]Aragón Institute of Engineering Research (I3A), [‡]Technological College of Huesca and [§]Institute of Nanoscience of Aragón (INA), University of Zaragoza, crta. Cuarte s/n, Huesca E-22071, Spain

[∥]Department of Materials and Environmental Chemistry, Stockholm University, SE-106 91 Stockholm, Sweden

KEYWORDS

Biochar; Slow Pyrolysis; Two-Phase Olive Mill Waste; Compost Refining Refuse; Pressure.

ABSTRACT

This work examines the effect of the absolute pressure (0.1 or 1.0 MPa) and the addition of a high-ash rejected material from municipal solid waste (MSW) composting (RC) on the slow pyrolysis of two-phase olive mill waste (OW). The experiments were conducted in a batch pyrolysis system using an initial mass of 750 g of feedstock. Three types of initial materials were tested: the OW alone, a mixture of OW and pure additives (5 % wt. of K_2CO_3 and 5% wt. of CaO) and a mixture of OW and RC (10 % wt.). For the OW without any additive, an increased pressure led to a market increase in the carbonization efficiency (i.e., fixed-carbon yield). At atmospheric pressure, the addition of either additives (CaO + K_2CO_3) or RC led to important changes in the pyrolysis behavior, due to the catalytic role of the alkali and alkaline Earth metals (AAEMs). However, this catalytic effect, which is translated into an enhancement of the decomposition of both the hemicellulose and cellulose fractions, was not observed at 1.0 MPa. The potential stability of all the produced biochars appeared to be very high, given the results obtained from both proximate and ultimate analysis. This high stability was confirmed by ^{13}C and ^{1}H solid-state NMR, which showed that the carbon contained in the biochars was composed mainly or entirely of highly condensed aromatic structures. However, the highest values of *stable C* (Edinburgh stability tool) and $R_{50,x}$ (recalcitrance index) were obtained for biochars produced from the OW+RC mixtures at any pressure . In summary, the addition of the rejected material from MSW composting appears to be a very cost-effective measure to obtain a potentially high-stable biochar, even at atmospheric pressure.

1. INTRODUCTION

The challenge of climate change mitigation has led to a growing interest in developing new technologies focused on increasing the carbon sinks and reducing greenhouse gas emissions.[1] Among the possible alternatives, pyrolysis of agricultural wastes appears to be a very promising option to integrate measures of carbon sequestration and generation of renewable energy into conventional agricultural production. The solid product from pyrolysis, called as biochar when it is incorporated into soils, is a predominantly organic and carbon-rich material, which can be effective for long-term carbon sequestration.[2]

Slow pyrolysis is commonly used to produce biochar, with gas as co-product. It is a relatively simple and robust process which can be applicable to small-scale and farm-based production of biochar.[3] Given the variability in the process conditions (e.g., heating rate may vary from 1 to 30 °C min^{-1}, whereas peak temperature usually ranges from 350 to 700 °C) in combination with a wide range of available biomass sources (with different inherent characteristics), a large variability can be expected in the properties of the produced biochars, and ultimately, in their ability to permanently sequester carbon in the soil.[4] Hence, one of the main challenges for the researching biochars is to appropriately relate the stability of biochar (a basic requirement for the use of biochar for the purpose of carbon sequestration) to the process conditions of pyrolysis for a given biomass feedstock.[5, 6]

The potential stability of biochars can be estimated from long-term incubation experiments.[7, 8] However, given that such experiments are extremely time consuming, a more practical approach is required.[9] In this sense, a number of techniques have been proposed to assess the long-term stability of biochar; for instance: (i) Enders et al.[10] proposed to use a combination of the content of volatile matter and the molar H:C and O:C ratios (e.g., biochars with low content of volatile

matter coupled to an H:C ratio below 0.4 and an O:C ratio below 0.2 may indicate high potential for carbon sequestration); (ii) Singh et al.[11] have reported significant correlations between the stability of the carbon in biochar (determined through medium- and long-term incubation experiments) and the aromaticity of biochar as determined by solid-state ^{13}C NMR spectroscopy; (iii) Harvey et al.[12] have proposed a recalcitrance index (R_{50}), which is based on the relative thermal stability of a given biochar to that of graphite; and (iv) an alternative method that uses H_2O_2 oxidation to accelerate the 'aging' and, hence, the oxidative loss of carbon from biochar has been developed by researchers from the UK Biochar Research Center.[13, 14]

Although the pyrolysis of biomass has been widely studied since many years, the number of studies focused on the effect of the absolute pressure on the pyrolysis of biomass is relatively modest. Moreover, the effect of a moderate pressure (0.5–5.0 MPa) has usually been measured as a combined effect with the gas residence time. In this sense, several of the earlier studies have reported on an increment of the char and gas yields, at the expense of tar (i.e., organic condensable fraction), when both the pressure and gas residence time had been increased.[15-20] However, other studies have found a negligible[21] or even negative[22, 23] effect of the absolute pressure on the yield of char. It is interesting to highlight that some of these works[20, 23] analyzed the effect of the pressure by keeping constant the residence time of the inert gas (N_2) within the pyrolysis reactor, as an attempt to clarify the pure effect of the pressure. Qian et al.[20] observed for the pyrolysis of rice husk in a fixed-bed reactor that the yields of char, water, and gas increased with elevating the pressure from 0.1 to 1.0 MPa at the expense of a reduction in the tar yield; however, these effects became insignificant when the pressure was elevated from 1.0 to 5.0 MPa. Manyà et al.[23] analyzed the effect of the absolute pressure (in a range of 0.1–1.0 MPa) on the pyrolysis of two-phase olive mill waste (OW) in a laboratory-scale fixed-bed reactor.

They reported on a statistically significantly decreased yield of char when the pressure was increased. To explain this decrease, the authors suggested that an increased pressure could enhance the kinetics of the steam gasification reaction. In any case, serious doubts still exist about the real effect of the absolute pressure on the distribution of the pyrolysis products. According to Elyounssi et al.[24], long residence times of the gas phase might be the main reason for the elevated yields of secondary char and gases, owing to the enhanced effects of secondary reactions involving volatile and chemically active species in the vicinity of the surface of the solid phase.

Lignocellulosic biomass and especially agricultural waste often contain relatively high contents of alkali and alkaline Earth metallic species (AAEMs), which can significantly alter the pyrolysis process. It is well recognized that high contents of AAEMs in biomass are generally associated with low temperatures required for pyrolysis, high yields of char and gas, and low levels of tar.[25, 26] The influence of added AAEMs on the biochar formation has also been reported in the literature.[27-29] For example, Wang et al.[28] observed an increase in the yields of gas and char with the physically added K_2CO_3 (17.7 wt. %) during the slow pyrolysis of pine wood. CaO has a catalytic effect on tar cracking.[30, 31] In this respect, Wang et al.[32] observed that by adding CaO to the pyrolysis of corncob, decarboxylation of organic acids was very effectively promoted, leading to the formation of light hydrocarbons. In addition, CaO is a good low cost sorbent for CO_2.

In a recent publication, Manyà et al.[33] have reported on a noticeable increase in the fixed-carbon yield (i.e., carbonization efficiency) for the pyrolysis of OW at 600 °C and atmospheric pressure with 10 wt. % of a rejected material from MSW composting (RC) in the physical mixture. The RC used was the reject fraction generated during the compost refining step in a

municipal solid waste (MSW) treatment plant, which employs a sequential process of anaerobic digestion of the organic fraction and subsequent aerobic composting. The RC had a high content of ash (72.5 wt. % in a dry basis) with relatively high levels of AAEMs. However, it should be highlighted that the experiments reported in the above-mentioned study[33] were conducted in a laboratory-scale fixed bed reactor using an initial sample mass of around 8 g. In that system, the diffusion rate of volatiles was relatively high and, hence, the extent of secondary charring reactions was modest. In other words, it would be interesting to analyze the role of the added RC in a bigger reactor and under certain operating conditions (e.g., under a moderate pressure) which can lead to the promotion of the secondary charring reactions resulting in very high carbonization efficiencies.

The specific aim of this study was to evaluate the effect of pressure as well as the addition of additives (a mixture of K_2CO_3 and CaO and the above-mentioned RC) on the pyrolysis of OW in a pressurized bench-scale fixed-bed reactor, which can process up to 1 kg of feedstock per batch. All pyrolysis tests have been conducted at a peak temperature of 600 °C, since we observed in an earlier study[23] that, for peak temperatures ranging from 400 to 600 °C, operating at the highest temperature led to the highest fixed-carbon yields, the lowest molar H:C and O:C ratios as well as the highest percentages of aromatic carbon in biochar. Special attention has been focused on the carbonization efficiency as well as on the properties of biochar related to its potential stability. The distribution of the pyrolysis products, the mass loss rate and the composition of the producer gas were also determined and compared in order to establish the influence of the tested operating conditions.

2. EXPERIMENTAL SECTION

2.1. Materials. The OW samples were supplied by an extra-virgin olive oil factory located in the Somontano region (Aragon, Spain). In that factory, two-phase olive mill wastes were sun-dried in the field for several months. The as-received material was broken in a jaw crusher and sieved to obtain a particle size in the range of 0.32–3.0 mm. Proximate analyses were conducted by quadruplicate according to ASTM standard D1762-84 to determine the ash content, volatile matter and fixed-carbon. Ultimate analyses were performed by triplicate using a Leco TruSpec Micro CHNS analyzer. The ash composition was measured using an ADVANT'XP+ XRF spectrometer (Thermo ARL, Switzerland) according to ASTM standard D4326-04. The results from characterization are given in Table 1.

Analytical reagent-grade K_2CO_3 and CaO were used as additives. Prior to use, the reagents were dried at 105 °C for 2 h and then sieved to discard the > 0.50 and < 0.074 mm fractions. Both reagents were directly added to the OW sample by dry mixing with mortar and pestle at a ratio of 10 wt. % (5% K_2CO_3, 5% CaO). The RC was crushed and sieved to obtain particles in the range of 0.15–1.2 mm. The results from the characterization of this material are also given in Table 1. The RC was also added to the OW sample at a ratio of 10 wt. %.

2.2. Pyrolysis System and Procedure. The fixed-bed pyrolysis system consists of a cylindrical and vertical reactor (140 mm ID; 465 mm long) made of Sandvik 253 MA™ stainless steel. This reactor was heated by two electric resistances of 2.1 kW with proportional integral derivative (PID) temperature control. The total volume was 6 L and a basket of 4 L made of Monel™ alloy was used to put the biomass into the reactor. The temperature inside of the bed was measured using four thermocouples placed into a thermowell (placed at a radius of 15 mm) in different heights, three in contact with the bed (bottom, middle and top) and one in the

freeboard (see Figure S-1 of the Supporting Information for further details). A back pressure regulator was used to maintain the pressure of the system at a desired value. The produced gas passed through a heated line, maintained at a temperature of around 280 °C, before being passed through a series of two glass traps that were immerged in ice-water baths. A schematic diagram of the whole experimental set-up is shown in Figure 1.

The pyrolysis tests were conducted under an atmosphere of nitrogen gas, the mass flow rate at NTP conditions of which was adjusted as a function of the absolute pressure (0.1 or 1.0 MPa) to maintain the real mass flow rate of nitrogen within the reactor (at 600 °C) at a constant value of 1.85 L min^{-1}. During the experiments, the sample was heated at an average heating rate of 5 °C·min^{-1} up to the peak temperature with a soaking time of 60 min at this temperature. The initial sample weight was 750 g, which represents around 70% of the basket volume with a bed height of around 270 mm. The pyrolysis reactor is supported on a ceramic tube of 117 mm OD and 330 mm long, which is placed on a weighing platform from Kern (model DS with a weighing range up 100 kg and a reading precision of 0.5 g). Flexible stainless steel tubes (460 mm in length, 10 mm OD) were used for the connections of the reactor to minimize any force component. A programmable logic controller (PLC) from Unitronics (model Vision 570) was used to control and collect the data (including the signal from the weighing platform).

After each experiment, the biochar present in the reactor was collected and weighed. The pyrolysis liquid was recovered directly from the condensers without using any solvent as wash liquid. The glass traps were weighted before and after each pyrolysis run to estimate the total mass of liquid. The water content of the pyrolysis liquid was determined by Karl-Fischer titration. The tar content was then determined by difference from the total mass of liquid. The composition of the major components in the pyrolysis gas (N_2, CO_2, CO, CH_4, C_2H_x and H_2) was

determined using a Varian micro gas chromatograph (model CP-4900) equipped with two analytical columns: a Molsieve 5A (using argon as carrier gas) and a PolarPlot Q (using helium as carrier gas).

All the pyrolysis runs were conducted at a constant peak temperature of 600 °C and under absolute pressures of 0.1 and 1.0 MPa. Three types of initial materials were tested: the OW alone (OW), the mixture of OW and pure additives (OW+A) and the mixture of OW and RC (OW+RC).

To verify whether the above-described experimental setup can produce reproducible and accurate results, a particular experimental run was performed five times. For these runs, 400 g of vine shoots were pyrolyzed at atmospheric pressure and at a peak temperature of 600 °C. The mass of produced gas was calculated from the N_2 content in the outlet gas stream, which was used as an internal standard. Mass balances were 97–99 wt. % and the mass yields of products were perfectly reproducible (char = 0.323 ± 0.9%; water = 0.288 ± 2.1%; tar = 0.155 ± 2.8%; gas = 0.215 ± 0.5%).

2.3. Characterization of the Biochar Product. Proximate and ultimate analyses were conducted for biochars applying the same procedures as described in section 2.1. The retention of carbon in biochar (C_{ret}) can be calculated as follows:

$$C_{ret}\,(\%) = y_{char}\left(\frac{C_{bc}}{C_{bio}}\right)100 \qquad (1)$$

where y_{char} is the mass yield of biochar in a dry and ash-free (daf) basis; whereas C_{bc} and C_{bio} corresponds to the carbon contents in a daf basis of biochar and feedstock, respectively. We note, however, that the carbon retention is not a reliable indicator of the carbonization efficiency. The reason is that carbon contained in the volatile matter of biochar is also counted as retained

carbon. Hence, the yield of fixed-carbon (y_{FC}) appears as a more convenient indicator of the carbonization efficiency and can be calculated according to eq 2.[6, 15]

$$y_{FC}\ (\%) = x_{FC,bc} \cdot y_{char} \cdot 100 \quad (2)$$

In eq 2, $x_{FC,bc}$ corresponds to the mass fraction of fixed-carbon in the biochar (in daf basis). The H:C and O:C ratios for the produced biochars were calculated from ultimate analysis data.

To measure the aromaticity of the biochars, solid-state ^{13}C magic angle spinning (MAS) NMR spectra were recorded on a 9.4 T Bruker Avance-III spectrometer (Larmor frequency of 100.6 MHz) equipped with a 7 mm double-resonance MAS probe. Spectra were recorded for samples spun at 5 and 7 kHz, and the chemical shift scale was externally calibrated using tetramethylsilane. The radio frequency (rf) pulse used for direct polarization (DP) experiments was calibrated with a sample of adamantane. A 45° flip angle rf pulse and a repetition delay of 360 s was used. For the cross polarization (CP) experiments, the repetition delay was 3 s, and cross polarization times of 0.8 and 2 ms were used. A moderately wide exponential function was applied to the recorded free-induction decays before the Fourier transformation. Solid-state ^{1}H NMR spectra were recorded on a 9.4 T Bruker Avance-III spectrometer equipped with a 7 mm double-resonance MAS probe with a spinning rate of 7 kHz and a repetition time of 20 s. Additional solid-state ^{1}H NMR spectra were recorded on a 14.1 T Bruker Avance-III spectrometer equipped with a 4 mm double-resonance MAS probe with a spinning rate of 14 kHz and a repetition delay of 13 s.

The specific surface area of the biochars was analyzed using N_2 physisorption data recorded at a temperature of −196 °C on a TriStar 3000 gas adsorption analyzer (Micromeritics, USA). The surface area (S_{BET}) was calculated using the Brunauer–Emmet–Teller model from adsorption

data obtained at relatively low relative pressures (0.05–0.20). The average pore diameter (d_{avg}) was calculated from the total pore volume and S_{BET}.

Temperature programmed oxidation (TPO) of the biochars was performed using a thermobalance (a MK2 microbalance with a readability of 0.1 μg from CI Precision, UK). 10 mg of each biochar sample was heated, in N_2-diluted air (10 mL min^{-1}), from room temperature to 950 °C at a linear heating rate of 10 °C min^{-1}. The raw TPO data were corrected for moisture and ash according to the procedure followed by Harvey et al.[12] The R_{50} index, which is related to the potential recalcitrance of the biochars, was calculated from the corrected TPO data using the following equation:[12]

$$R_{50,x} = T_{50,x} / T_{50,g} \tag{3}$$

where $T_{50,x}$ and $T_{50,g}$ are the temperatures corresponding to 50% of mass loss of biochar x and graphite, respectively.

Direct oxidation of biochars was conducted following the same procedure described by Cross and Sohi (Edinburgh stability tool).[13] Biochar samples containing 0.1 g C were milled to a fine powder in a ball mill and then treated in a test tube with 7 ml of an aqueous solution of H_2O_2 (5% H_2O_2), initially at room temperature and then at 80 °C for 48 h. The samples were then dried in an oven at 105 °C overnight. The "stable C" was expressed as the percentage of the initial 0.1 g C that remains after oxidation, assessed from the gravimetric mass loss and measurements of the C contents before and after oxidation. Each biochar sample was measured three times.

3. RESULTS AND DISCUSSION

3.1. Weight Loss Profiles. The normalized mass-loss and its time derivative curves for each experiment are displayed in Figures S-2–S-7 (Supporting Information). In the same Figures, the axial temperature profiles (see Figure S-1 for the detailed position of thermocouples) are also

given. To compensate for the buoyancy effect of the surrounding air, three blank tests were conducted (using the same heating protocol as in the pyrolysis tests) to obtain the background of the signal. For each pyrolysis experiment, the background signal was subtracted to obtain the final results. Results from the three blank tests showed a good degree of reproducibility, as illustrated in Figure S-8.

Figure 2 compares the mass-loss derivative curves obtained from the experiments. As expected, the addition of either additives ($CaO + K_2CO_3$) or RC led to important changes in the pyrolysis behavior. At atmospheric pressure, the highest mass-loss rate was increased and shifted to lower temperatures in the presence of additives and RC. This catalytic effect could mainly be attributed to the relatively high levels of K, which promotes the decomposition of the hemicellulose and cellulose fractions as has been reported in earlier studies.[34, 35] As a result, the peaks corresponding to hemicellulose plus extractives (mainly some olive oil retained in the OW) and cellulose were merged in Figure 2b. This finding could also indicate that the dry mixing of OW and metal compounds used here was adequate enough to allow the mobility of K on the char. In fact, Karimi and Gray[36] already reported a high mobility of potassium within the char phase when K_2CO_3 was physically mixed with bitumen coke at a ratio of 27.5 wt. %. The minor peaks appearing at higher temperatures (time > 200 min) for the pyrolysis of OW could be related to a delayed decomposition of the lignin fraction, given the existing high temperature gradients. For the pyrolysis of OW+A and OW+RC, these minor peaks could correspond to a catalyzed decomposition of the fraction of lignin that decomposes at high temperature. An additional potential explanation for the mass loss at high temperature could be related to some calcination of hydroxides and carbonates (e.g., $Ca(OH)_2$ and $CaCO_3$ produced from the

adsorption of H_2O and CO_2 on CaO for experiments conducted using the OW+A mixtures), which can start at temperatures of 450–500 °C[37] and 600–650 °C[31, 32], respectively.

However, the behavior under a moderate pressure of 1.0 MPa was found to be different. The above-mentioned increases in the devolatilization rate with additives (and RC) were not observed for the pressurized pyrolysis. In fact and compared to the pressurized pyrolysis of OW, a comparably lower highest rate (in the case of RC) and/or a shift of the major peak to higher temperature (for pure additives) can be seen in Figure 2. Qian et al.[20] suggested that an increase in pressure (from 0.1 to 5.0 MPa) can promote the decarboxylation of both hemicellulose and cellulose during the pyrolysis of rice husk. In line with this study, Manyà et al.[22] reported on a significantly decreased temperature for the highest mass-loss when the absolute pressure was increased from 0.1 to 1.0 MPa in a pressurized thermogravimetric analyzer. This trend was only observed for the experiments conducted using OW alone. The unexpected behavior for both the OW+A and OW+RC mixtures could be related to that an increased pressure may alter the fates and roles of the AAEMs during pyrolysis. In this sense, it can be hypothesized that pressure could inhibit the migration of the K species into the char. According to Karimi and Gray[36], the formation of potassium intercalate-like structures in condensed aromatic layers of carbon seems to be the main explanation for the mobility of K. Under pressurized conditions, however, K could be present in the form of different compounds with lower mobility, as firstly suggested by Bruno et al.[38] Scanning electron microscopy and energy dispersive X-ray spectrometry (SEM/EDX, Inspect F50, FEI Europe, the Netherlands) was used to analyze the dispersion of the inorganics in the chars. The results from the SEM/EDX analyses, which are summarized in Table S-1 (Supporting Information), seem to confirm the above-mentioned assumption, since they reveal that the contents of K in the biochars obtained by pressurized pyrolysis of OW+A and

OW+RC mixtures were much lower than those measured for the biochars produced from the same starting materials at 0.1 MPa.

3.2. Distribution of the Pyrolysis Products. The yields of biochar (y_{char}), produced water (y_{water}), tar (y_{tar}) and gas (y_{gas}) (all of them expressed in a daf basis; y_{gas} calculated by difference) are graphically summarized in Figure 3. Several observations can be made from the results given in Figure 3. At any pressure, but especially at 0.1 MPa, the addition of either chemicals or RC led to a decrease in the biochar yield. These decreases are consistent with the higher mass-loss rates shown in Figure 2b and indicate that the formation of both primary and secondary char could not sufficiently be promoted by the AAEMs. One possible explanation for this is that the dry-blending method used to prepare the mixtures was not sufficiently effective for this purpose. In this context, Hayashi et al.[39] observed that the addition of $Mg(OH)_2$, $Ca(OH)_2$ and NaOH to mixtures of biomass and PVC using the dry-blending method did not cause any significance change in the biochar yield after pyrolysis at peak temperatures of 300, 400 and 500 °C. The authors pointed out that a wet-blending method (i.e., by soaking the biomass sample in an aqueous solution of the given salt) was needed to clearly observe the effect of additives on the biochar yield. The fact that we used a dry and ash-free basis, to exclude the inherent and added inorganic constituents, can additionally explain the lower values of y_{char} reported here for the OW+A and OW+RC mixtures.

The effect of pressure on the biochar yield seems to be relatively modest (see Figure 3a), except for the case of pure OW samples, where a decrease in y_{char} was observed when the pressure was increased. This could be explained by a certain enhancement of the kinetics of the steam gasification reaction leading to non-negligible reaction rates, even at relatively low temperatures.[23] The decrease in the biochar yield may seem to be in disagreement with some

earlier studies, which have reported on a higher production of biochar when the pressure was increased.[15, 16, 18, 19] Nevertheless, note that these studies were conducted at a constant mass flow rate of inert gas and, thus, the gas residence time increased as the pressure rose. Consequently, the observed increases in the char yield could exclusively be related to the longer times for vapor-solid contact that occurred on the increased pressure.

For the pyrolysis of both OW+A and OW+RC samples, increasing the absolute pressure from 0.1 to 1.0 MPa resulted in a decreased production of water and tar at the expense of a higher production of gas. In other words, increasing the pressure could enhance the kinetics of the tar cracking and reforming reactions in the freeboard region.

The addition of RC to the pyrolysis of OW led to a marked decrease in the tar yield. Under an absolute pressure of 1.0 MPa, the tar yield was further decreased as compared with a pressure of 0.1 MPa, leading to higher yields of gas. Assuming a scenario where the pyrolytic tars are taken as unwanted by-products, the RC tested here appears to be a suitable and cost-effective additive for biomass pyrolysis.

3.3. Yields of Gaseous Species. The release profiles of the main gases are shown in Figure S-9. It can be seen that CO_2 and CO were the first two gases to evolve, followed by C_2H_x, CH_4 and H_2. The initial formation of CO_2 and CO can be mainly due to the decarboxylation and decarbonylation of hemicellulose and extractives[20], whereas the release of these gases from cellulose required higher temperatures, especially during the pyrolysis of OW at atmospheric pressure. As already mentioned above, the addition of AAEM compounds and/or an increase in the pressure can promote the decomposition of both the hemicellulose and cellulose fractions leading to a faster release of both CO_2 and CO.

The cumulative yields of the main gaseous species are shown in Figure 4. The yield of CO_2 was enhanced with the increased pressure, regardless of the starting material used. High pressure also led to an increased yield of CH_4 and a decreased yield of CO. These trends are in full agreement with those reported by Qian et al.[20] for the pressurized pyrolysis of rice husk. Table 2 lists the main homogeneous (vapor phase) and heterogeneous (solid-vapor phase) reactions that can occur during the release of the produced gas. From a thermodynamics point of view, an increased pressure favors the production of CO_2 through reactions 2 and 6. The production of CH_4 via reactions 3, 4 and 6 is also favored by higher pressure. For reactions 2, 3 and 6; the enhanced production of CO_2 and/or CH_4 occurs at the expense of consumption of CO. In addition, the rate of CO conversion during the water-gas shift (WGS) reaction (reaction 1 in Table 2) is expected to increase with raising the total pressure, as was already observed by Hla et al.[40] The enhancement in the kinetics of the WGS reaction at high pressure could explain why the yield of H_2 did not decrease as much as the yield of CO.

On the other hand, the added AAEMs (for both OW+A and OW+RC mixtures) could enhance the production of H_2 by promoting reaction 1 (as has recently been reported by Hu et al.[41]) and, to a lesser extent, reaction 5 (see Table 2). Additional H_2 can also be produced through dehydrogenation of volatiles, which is promoted by the AAEMs in the bed and freeboard region. In the case of using K_2CO_3 and CaO as additives, the yield of CO also increased considerably, probably as a consequence of the catalytic role of K on the decarbonylation reactions.[28] Concerning the yield of CO_2, the relatively low values for both OW+A and OW+RC samples at 0.1 MPa can be explained by the adsorption of CO_2 on CaO to form $CaCO_3$. However, the addition of AAEMs under pressurized conditions did not result in any apparent decrease in the cumulative yield of CO_2, in spite of that an increased pressure thermodynamically favors the

carbonation of CaO.[42] This finding can suggest that the extra amount of CO_2 produced by an enhancement of the direct WGS reaction rates at high pressure was larger than that adsorbed on CaO.

3.4. Characteristics of the Biochars. Table 3 lists the values for each biochar of C_{ret}, y_{FC}, molar H:C and O:C ratios, $R_{50,x}$, *stable C* (according to the Edinburgh stability tool[13]) as well as the specific surface area (S_{BET}) and average pore diameter (d_{avg}). The highest carbonization efficiency (i.e., y_{FC}) was observed for the pressurized pyrolysis of the olive mill waste without any additive. Under pressure, the lower production of biochar as compared with the non-pressurized pyrolysis was compensated by an increased content of fixed-carbon. For both OW+A and OW+RC samples, the carbonization efficiency was not appreciably affected by the absolute pressure (both the y_{FC} and $x_{FC.bc}$ values were very similar for biochars produced at 0.1 and 1.0 MPa).

From Table 3, it can also be seen that the molar H:C and O:C ratios were very low in all cases (less than 0.4 and 0.1, respectively). According to the preliminary classification proposed by Enders et al.[10], which is mainly based on the values of these ratios, the biochars produced here appear to have a high carbon sequestration potential (i.e., high potential stability).

Figure 5 summarizes solid-state ^{13}C DP and ^{13}C CP NMR spectra for all samples as acquired at a MAS frequency of 7 kHz. The ^{13}C DP spectra report on all carbon atoms while signals in a ^{13}C CP spectrum are enhanced for carbons with hydrogens nearby, due to the proton magnetization transfer. All ^{13}C NMR spectra showed similar features, in particular a broad signal at a chemical shift of ≈128 ppm, which was assigned to aromatic carbon. Furthermore, for the biochars produced from the OW+A mixtures, the ^{13}C DP spectra displayed a carbonate peak at a chemical shift of 168 ppm, which indicates that $CaCO_3$ was not or only partly calcined,

regardless of the pressure applied. No ^{13}C CP spectrum could be recorded for the OW+A-derived biochar at 1.0 MPa. One reason for this absence might be that the proton magnetization had already decayed during the CP duration, which cancels the desirable enhancement. The MAS rate for the ^{13}C CP NMR measurements was varied to move sidebands away from the aliphatic region (i.e., 30–70 ppm), but no aliphatic carbon atoms were observed. However, the ^{1}H NMR spectra in Figure 6 displayed some signatures of aliphatic carbons. This apparent inconsistency most probably relate to that some aromatic protons relax very rapidly or have very broad corresponding ^{1}H NMR spectra. All those spectra had showed a broad peak between 0 and 1.5 ppm arising most likely from ^{1}H atoms bonded to saturated carbons. The spectrum for biochar produced from OW at 0.1 MPa showed an additional sharp peak at 1.9 ppm, which could correspond to a ^{1}H atom bonded to an unsaturated carbon (some aliphatic features not detectable in ^{13}C NMR). The aromatic groups are highly condensed and no detectable signals in the typical ^{1}H region were detected. In the case of the biochar produced from OW at 0.1 MPa, the spectrum recorded at 14 kHz (green line) showed a small peak at a chemical shift of ≈5.9 ppm, which was tentatively assigned to aromatic groups with high mobility and/or being isolated from nearby protons.

In summary, the results from the solid-state ^{13}C and ^{1}H NMR characterization indicate a very high degree of aromaticity of the biochars. With the exception of the biochar produced without any additive at atmospheric pressure, all the carbon contained in the biochars was aromatic. Assuming the strong direct correlation between the content of aromatic carbon and the carbon stability in soil, which has been found by Singh et al.[11], we must highlight the high potential stability of the biochars produced here.

The $R_{50,x}$ values reported in Table 3 ranged from 0.506 to 0.635, indicating that biochars can be classified as class B (i.e., carbons exhibiting a reduced susceptibility to biodegradation) according to the classification proposed by Harvey et al.[12] It is interesting to note that the highest $R_{50,x}$ values were obtained for the OW+RC mixtures. The relatively low values obtained for the biochars produced from OW+A mixtures can be explained by an additional mass loss due to the decomposition of $CaCO_3$ at high temperatures. This fact, which is clearly shown in Figure 7, can lead to an underestimation of the R_{50} index when CaO is used as an additive.

The results obtained for the percentage of stable C (Edinburgh stability tool) showed a similar trend as the results of $R_{50,x}$. The highest values were also obtained for the OW+RC mixtures (see Table 3). At this point, it becomes interesting to jointly analyze the variables related to the potential stability ($x_{FC,bc}$; molar H:C and O:C ratios; $R_{50,x}$; and *stable C*) by Principal Component Analysis (PCA), which allows clustering of observations and variables on the basis of their correlations and variances.[43] More in detail, PCA seeks to maximize the variance of a linear combination of the initial variables. It should be noted that none of the variables is designated as dependent, and no grouping of observations can be assumed. The plot of the first two components (score plot) can reveal important features of the data set, such as a tendency of the individuals (biochar samples in the present study) to cluster. For its part, the loading plot reveals the relationships between the original variables in the space of the two first components. For this study, PCA was applied to the correlation matrix in order to normalize all the variables (i.e., each variable will contribute equally). From the bi-plot (combined score and loading plots) displayed in Figure 8, it can be seen that the molar H:C ratio and the fixed-carbon content ($x_{FC,bc}$) are highly correlated (an angle of 180 degrees between the lines). In addition, the variables $R_{50,x}$ and *stable C* appear to be correlated among them but highly uncorrelated with the rest of variables. In

other words, predicting biochar stability only based on indicators derived from proximate and ultimate analysis can be not sensitive enough.

Regarding the BET specific surface areas listed in Table 3, they were very low as compared to those measured for other biomass-derived chars at similar peak temperatures.[44, 45] Further activation steps at temperatures higher than 600 °C, or by chemical activation methods, will be required to obtain biochars with higher specific surface areas. In fact, Pellera and Gidarakos[46] have reported a significant increase in the BET specific surface area when the pyrolysis peak temperature was increased from 400 to 700 °C (1.76 and 72.8 $m^2\ g^{-1}$, respectively) for an olive waste similar to that studied here.

4. CONCLUSIONS

Based on the results presented above, the following conclusions are derived:

(1) For the slow pyrolysis of OW alone, working at a moderate pressure (1.0 MPa) instead of an atmospheric pressure resulted in a marked increase in the carbonization efficiency. In other words, the biochar produced through pressurized pyrolysis retained more organic carbon (initially contained in the feedstock) as fixed-carbon as compared to the biochar produced under atmospheric pressure.

(2) At atmospheric pressure, the addition of either additives ($CaO + K_2CO_3$) or RC led to important changes in the pyrolysis behavior, due to the catalytic role of the AAEMs. However, this catalytic effect, which is translated into an enhancement of the decomposition of both the hemicellulose and cellulose fractions, was not observed at 1.0 MPa. One reason could be that pressure inhibits the mobility of the potassium species within the char phase.

(3) The RC tested in this study has been proved to be an effective additive for the pyrolysis of OW. With RC, the yields of H_2 and CH_4 were increased and the tar yield was decreased in

comparison with the pyrolysis of OW alone at any pressure. The carbonization efficiency was also improved by the addition of RC at atmospheric pressure.

(4) The potential stability of all the produced biochars appeared to be very high, since the values of the molar H:C and O:C ratios were lower than 0.4 and 0.1, respectively. This high stability was confirmed by the results of the solid-state ^{13}C and ^{1}H NMR, which showed that the carbon contained in the biochars was composed mainly or entirely of highly condensed aromatic structures. Some aliphatic features were only observed for the biochar produced from the OW alone at atmospheric pressure. We must highlight that the highest values of *stable C* (Edinburgh stability tool) and $R_{50,x}$ (recalcitrance index) were obtained for the biochars produced from the OW+RC mixtures at any pressure.

(5) Considering the effects of the addition of the RC on the carbonization efficiency, gas composition, tar yield and stability of the produced biochars and also that pressure plays a negligible role during the pyrolysis of OW+RC mixtures; we can conclude that the co-pyrolysis of OW and RC (with high ash content) at atmospheric pressure is a very promising cost-effective route.

ASSOCIATED CONTENT

Supporting Information. The location of thermocouples at different axial positions in the fixed bed reactor is shown in Figure S-1. The normalized mass-loss and its time derivative curves for each experiment are displayed in Figures S-2–S-7. Figure S-8 shows the impact of the buoyancy effect on the measured weight. Table S-1 summarizes the results obtained from the SEM/EDX analyses. Finally, the release profiles of the main gases for all runs are shown in Figure S-9.

AUTHOR INFORMATION

Corresponding Author

*E-mail: joanjoma@unizar.es

Notes

The authors declare no competing financial interest.

ACKNOWLEDGEMENTS

We dedicate this article to the memory of Prof. Michael J. Antal Jr., an enthusiastic researcher and a beloved friend. The authors wish to acknowledge financial support from the Spanish MINECO-DGI (Project ENE2013-47880-C3-1-R). JJM also express his gratitude to the Aragon Government (GPT group) and the European Social Fund for additional financial support.

ABBREVIATIONS

AAEM = alkali and alkaline Earth metals

CP = cross polarization

C_{ret} = carbon initially contained in the feedstock that remains in the biochar (%)

C_{bc} = carbon content in a daf basis of biochar (%)

C_{bio} = carbon content in a daf basis of OW (%)

d_{avg} = average pore diameter (nm)

DP = direct polarization

MAS = magic angle spinning

MSW = municipal solid waste

NMR = Nuclear Magnetic Resonance

NPCs = normalized principal components

OW = two-phase olive mill waste

$R_{50,x}$ = recalcitrance index for a given biochar x

RC = rejected material from MSW composting

S_{BET} = Brunauer–Emmet–Teller specific surface area ($m^2\ g^{-1}$)

SEM/EDX = Scanning Electron Microscopy and Energy Dispersive X-ray Spectrometry

$x_{FC,bc}$ = mass fraction of fixed-carbon in the biochar (in a daf basis)

y_{char} = biochar yield in a dry and ash-free basis (–)

y_{FC} = fixed-carbon yield in a dry and ash-free basis (%)

y_{gas} = yield of produced gas in a dry and ash-free basis (–)

y_{tar} = tar yield in a dry and ash-free basis (–)

y_{water} = yield of produced water in a dry and ash-free basis (–)

REFERENCES

(1) Li, F.; Cao, X.; Zhao, L.; Wang, J.; Ding, Z. *Environ. Sci. Technol.* **2014**, *48*, 11211–11217.

(2) Lehmann, J. *Nature* **2007**, *447*, 143–144.

(3) Song, W.; Guo, M. *J. Anal. Appl. Pyrolysis* **2012**, *94*, 138–145.

(4) Manyà, J. J. *Environ. Sci. Technol.* **2012**, *46*, 7939–7954.

(5) Mašek, O.; Brownsort, P.; Cross, A.; Sohi, S. *Fuel* **2013**, *103*, 151–155.

(6) Ronsse, F.; van Hecke, S.; Dickinson, D.; Prins, W. *GCB Bioenergy* **2013**, *5*, 104–115.

(7) Keith, A.; Singh, B.; Singh, B. P. *Environ. Sci. Technol.* **2011**, *45*, 9611–9618.

(8) Zimmerman, A. R. *Environ. Sci. Technol.* **2010**, *44*, 1295–1301.

(9) McBeath, A. V.; Smernik, R. J.; Krull, E. S.; Lehmann, J. *Biomass Bioenergy* **2014**, *60*, 121–129.

(10) Enders, A.; Hanley, K.; Whitman, T.; Joseph, S.; Lehmann, J. *Bioresour. Technol.* **2012**, *114*, 644–653.

(11) Singh, B. P.; Cowie, A. L.; Smernik, R. J. *Environ. Sci. Technol.* **2012**, *46*, 11770–11778.

(12) Harvey, O. R.; Kuo, L.; Zimmerman, A. R.; Louchouarn, P.; Amonette, J. E.; Herbert, B. E. *Environ. Sci. Technol.* **2012**, *46*, 1415–1421.

(13) Cross, A.; Sohi, S. P. *GCB Bioenergy* **2013**, *5*, 215–220.

(14) Crombie, K.; Masek, O.; Sohi, S. P.; Brownsort, P.; Cross, A. *GCB Bioenergy* **2013**, *5*, 122–131.

(15) Antal, M. J.; Allen, S. G.; Dai, X.; Shimizu, B.; Tam, M. S.; Gronli, M. *Ind. Eng. Chem. Res.* **2000**, *39*, 4024–4031.

(16) Rousset, P.; Figueiredo, C.; De Souza, M.; Quirino, W. *Fuel Process. Technol.* **2011**, *92*, 1890–1897.

(17) Antal, M. J.; Croiset, E.; Dai, X.; DeAlmeida, C.; Mok, W. S.; Niclas, N.; Richard, J. R.; Al Majthoub, M. *Energy Fuels* **1996**, *10*, 652–658.

(18) Noumi, E. S.; Blin, J.; Valette, J.; Rousset, P. *Energy Fuels* **2015**, *29*, 7301–7308.

(19) Recari, J.; Berrueco, C.; Abelló, S.; Montané, D.; Farriol, X. *Bioresour. Technol.* **2014**, *170*, 204–210.

(20) Qian, Y.; Zhang, J.; Wang, J. *Bioresour. Technol.* **2014**, *174*, 95–102.

(21) Melligan, F.; Auccaise, R.; Novotny, E. H.; Leahy, J. J.; Hayes, M. H. B.; Kwapinski, W. *Bioresour. Technol.* **2011**, *102*, 3466–3470.

(22) Manyà, J. J.; Roca, F. X.; Perales, J. F. *J. Anal. Appl. Pyrolysis* **2013**, *103*, 86–95.

(23) Manyà, J. J.; Laguarta, S.; Ortigosa, M. A.; Manso, J. A. *Energy Fuels* **2014**, *28*, 3271–3280.

(24) Elyounssi, K.; Blin, J.; Halim, M. *J. Anal. Appl. Pyrolysis* **2010**, *87*, 138–143.

(25) Raveendran, K.; Ganesh, A.; Khilar, K. C. *Fuel* **1995**, *74*, 1812–1822.

(26) Di Blasi, C.; Galgano, A.; Branca, C. *Energy Fuels* **2009**, *23*, 1045–1054.

(27) Jensen, A.; Dam-Johansen, K.; WÃ³jtowicz, M. A.; Serio, M. A. *Energy Fuels* **1998**, *12*, 929–938.

(28) Wang, Z.; Wang, F.; Cao, J.; Wang, J. *Fuel Process. Technol.* **2010**, *91*, 942–950.

(29) Nowakowski, D. J.; Jones, J. M.; Brydson, R. M. D.; Ross, A. B. *Fuel* **2007**, *86*, 2389–2402.

(30) Zhao, B.; Zhang, X.; Chen, L.; Sun, L.; Si, H.; Chen, G. *Bioresour. Technol.* **2014**, *156*, 78–83.

(31) Han, L.; Wang, Q.; Ma, Q.; Yu, C.; Luo, Z.; Cen, K. *J. Anal. Appl. Pyrolysis* **2010**, *88*, 199–206.

(32) Wang, D.; Xiao, R.; Zhang, H.; He, G. *J. Anal. Appl. Pyrolysis* **2010**, *89*, 171–177.

(33) Manyà, J. J.; García-Ceballos, F.; Azuara, M.; Latorre, N.; Royo, C. *Fuel Process. Technol.* **2015**, *140*, 276–284.

(34) Di Blasi, C.; Galgano, A.; Branca, C. *Ind. Eng. Chem. Res.* **2009**, *48*, 3359–3369.

(35) Shah, M. H.; Deng, L.; Bennadji, H.; Fisher, E. M. *Energy Fuels* **2015**, *29*, 7350–7357.

(36) Karimi, A.; Gray, M. R. *Fuel* **2011**, *90*, 120–125.

(37) Zhou, C.; Stuermer, T.; Gunarathne, R.; Yang, W.; Blasiak, W. *Fuel* **2014**, *122*, 36–46.

(38) Bruno, G.; Carvani, L.; Passoni, G. *Fuel* **1986**, *65*, 1368–1370.

(39) Hayashi, S.; Amano, H.; Niki, T.; Yokota, M.; Mae, K. *Ind. Eng. Chem. Res.* **2010**, *49*, 11825–11831.

(40) Hla, S. S.; Duffy, G. J.; Morpeth, L. D.; Cousins, A.; Roberts, D. G.; Edwards, J. H. *Catal. Commun.* **2009**, *11*, 272–275.

(41) Hu, S.; Jiang, L.; Wang, Y.; Su, S.; Sun, L.; Xu, B.; He, L.; Xiang, J. *Bioresour. Technol.* **2015**, *192*, 23–30.

(42) Lin, S.; Harada, M.; Suzuki, Y.; Hatano, H. *Energy Fuels* **2003**, *17*, 602–607.

(43) Hardle, W.; Simar, L. *Applied Multivariate Statistical Analysis; Statistical Series;* Springer: New York, 2003; Vol. 1.

(44) Jimenez-Cordero, D.; Heras, F.; Alonso-Morales, N.; Gilarranz, M. A.; Rodriguez, J. J. *Biomass Bioenergy* **2013**, *54*, 123–132.

(45) Lee, Y.; Park, J.; Ryu, C.; Gang, K. S.; Yang, W.; Park, Y.; Jung, J.; Hyun, S. *Bioresour. Technol.* **2013**, *148*, 196–201.

(46) Pellera, F.; Gidarakos, E. *J. Environ. Chem. Eng.* **2015**, *3*, 1163–1176.

Table 1. Proximate, Elemental, and XRF Analyses of the OW and RC Samples

Proximate (wt %)	OW	RC
Moisture	12.8 ± 0.12	17.4 ± 1.6
Ash	1.98 ± 0.11	59.9 ± 1.4
Volatile Matter	76.3 ± 2.98	18.8 ± 1.1
Fixed-Carbon	8.92 ± 1.13	3.90 ± 0.85
Ultimate (wt. %)[a]	OW	RC
C	50.0 ± 0.48	47.6 ± 0.62
H	6.21 ± 0.17	5.31 ± 0.05
N	2.29 ± 0.09	2.12 ± 0.02
S	0.40 ± 0.07	0.38 ± 0.01
O[b]	41.1 ± 0.66	44.6 ± 0.82
Inorganic matter expressed as percentage of oxides (wt. % of ash)	OW	RC
CaO	43.3 ± 0.25	30.8 ± 0.23
K_2O	33.7 ± 0.24	3.34 ± 0.09
SiO_2	4.34 ± 0.10	37.4 ± 0.24
P_2O_5	4.33 ± 0.10	3.16 ± 0.09
S (inorganic)	4.26 ± 0.10	3.82 ± 0.10
Fe_2O_3	2.91 ± 0.08	4.18 ± 0.10
MgO	1.65 ± 0.14	3.26 ± 0.09
Al_2O_3	1.60 ± 0.07	5.91 ± 0.12
PbO	0.55 ± 0.06	0.21 ± 0.01
Cl	0.37 ± 0.02	2.02 ± 0.07
Na_2O	ND[c]	4.31 ± 0.16

[a] Dry and ash-free basis

[b] Oxygen content calculated by difference

[c] Not detected

Table 2. Main Reactions during the Release of the Pyrolysis Gas

No.	Reaction	ΔG^d (kJ mol^{-1})	
		600 °C and 0.1 MPa	600 °C and 1.0 MPa
1	$H_2O + CO \rightleftharpoons CO_2 + H_2$	–0.2794	–0.2594
2	$2CO \rightleftharpoons CO_2 + C$	–1.648	–2.675
3	$3H_2 + CO \rightleftharpoons CH_4 + H_2O$	12.43	–10.29
4	$C + 2H_2 \rightleftharpoons CH_4$	2.758	–14.05
5	$C + H_2O \rightleftharpoons CO + H_2$	–0.0604	1.486
6	$2H_2 + 2CO \rightleftharpoons CO_2 + CH_4$	10.99	–26.06

[d] Calculated by Aspen Plus 8.8 using Peng-Robinson method and the Equilibrium Reactor (R_{equil}) module. The initial concentration in molar fraction of reactants and products was taken equal to *1/n*, where *n* is the number of species involved.

Table 3. Main Characteristics of the Produced Biochars

Run	C_{ret} (%)	y_{FC} (%)	$x_{FC,bc}$	H:C molar ratio	O:C molar ratio	$R_{50,x}$	Stable C[j] (%)	S_{BET} (m^2 g^{-1})	d_{avg} (nm)
OW at 0.1 MPa	58.46	23.13	0.616	0.3398	0.0324	0.564	89.4 ± 4.4	0.703	6.24
OW at 1.0 MPa	51.40	30.50	0.946	0.2985	0.0166	0.605	86.3 ± 1.3	1.74	0.731
OW+A at 0.1 MPa	41.38	26.88	0.946	0.3080	0.0921	0.506	82.9 ± 0.1	0.256	16.7
OW+A at 1.0 MPa	43.10	28.30	0.947	0.3350	0.0919	0.559	81.9 ± 4.5	0.639	11.9
OW+RC at 0.1 MPa	46.51	28.64	0.906	0.2524	0.0830	0.634	94.6 ± 1.5	4.62	2.92
OW+RC at 1.0 MPa	48.21	28.94	0.926	0.3979	0.0332	0.635	95.1 ± 1.0	1.40	4.83

[j] Percentage of carbon that remains in the biochar after H_2O_2 oxidation.

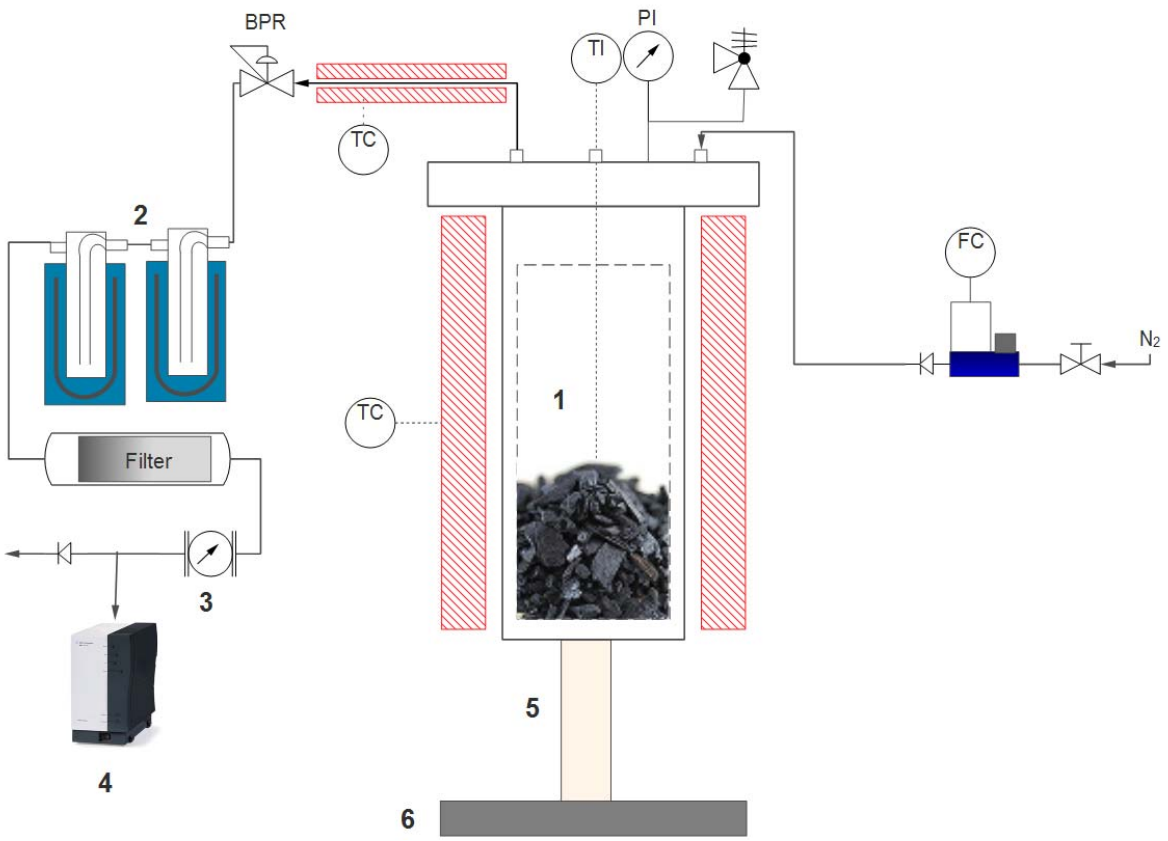

Figure 1. Schematic layout of the experimental device: (1) fixed-bed pyrolysis reactor, (2) pyrolysis liquid condensation system, (3) volumetric gas meter, (4) μ-GC, (5) ceramic tube, and (6) weighing platform.

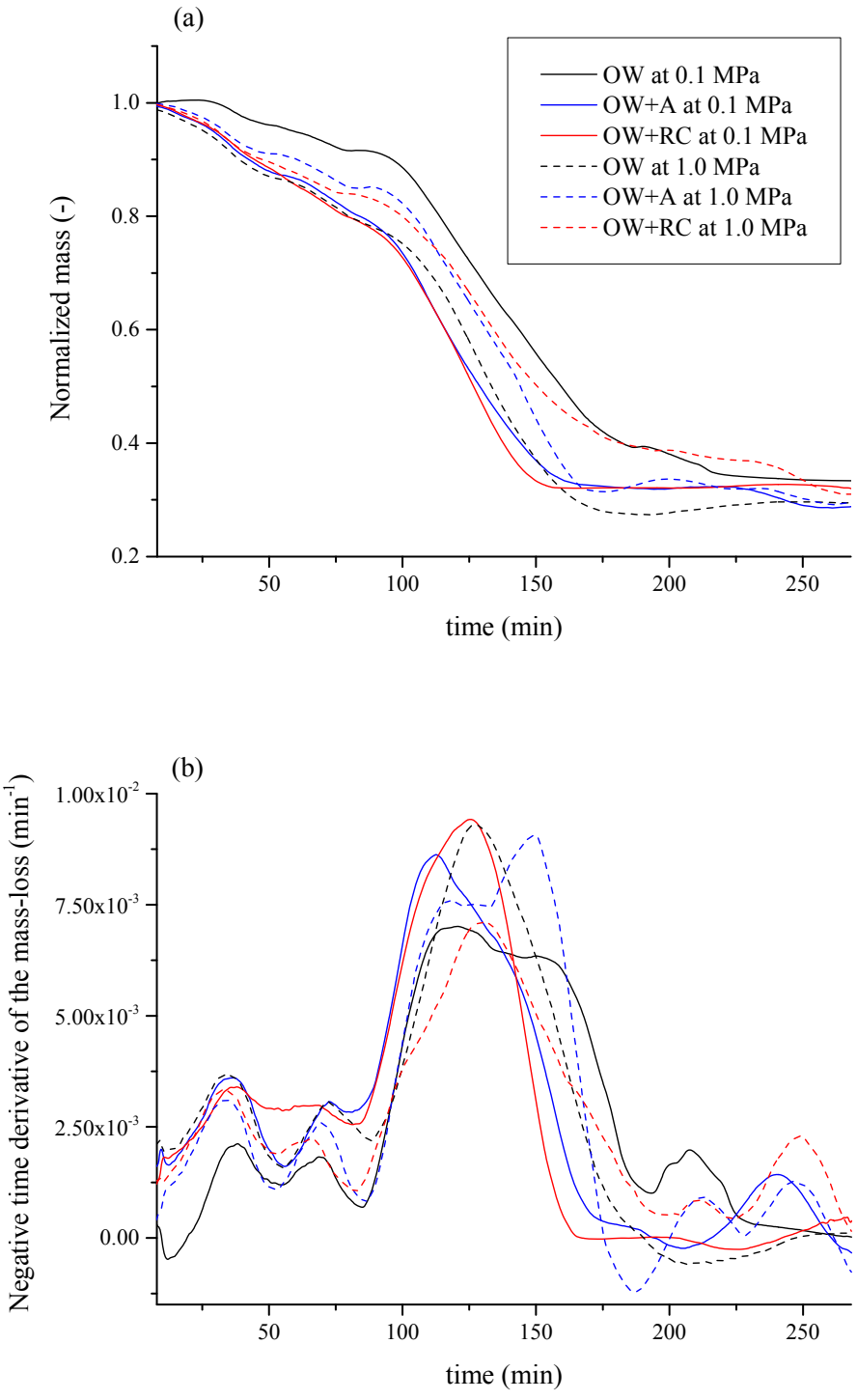

Figure 2. (a) Mass-loss and (b) negative time derivative of the mass-loss curves obtained for the pyrolysis runs.

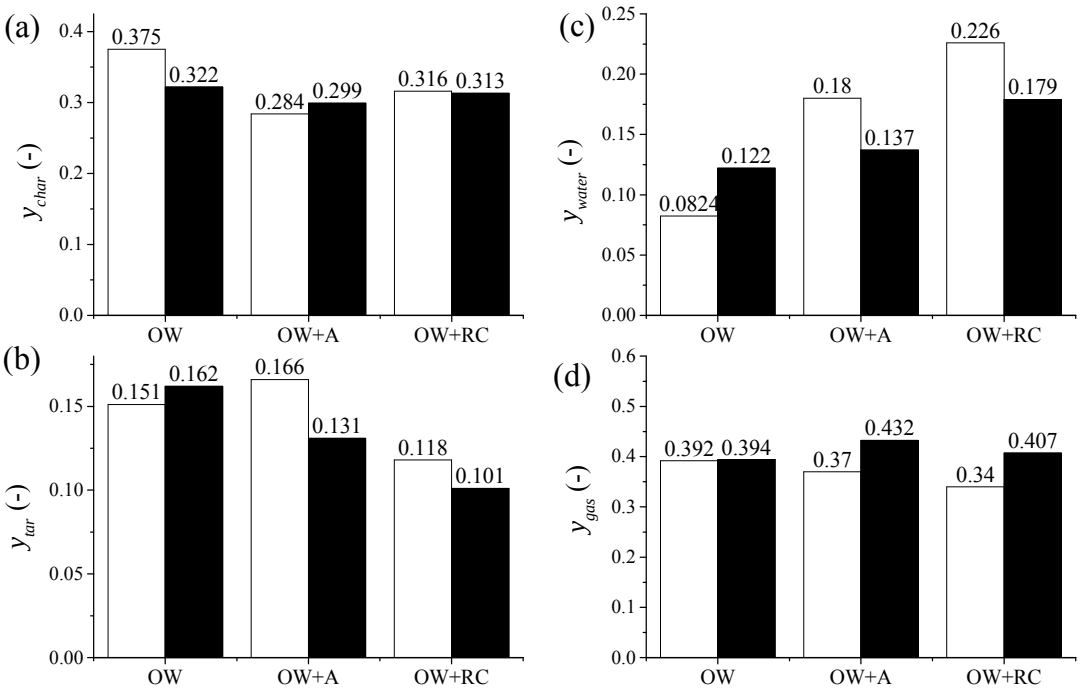

Figure 3. Mass yields (on a daf basis) of (a) char, (b) tar, (c) produced water, and (d) gas. White columns correspond to pyrolysis runs at 0.1 MPa, whereas black columns refer to runs conducted at 1.0 MPa.

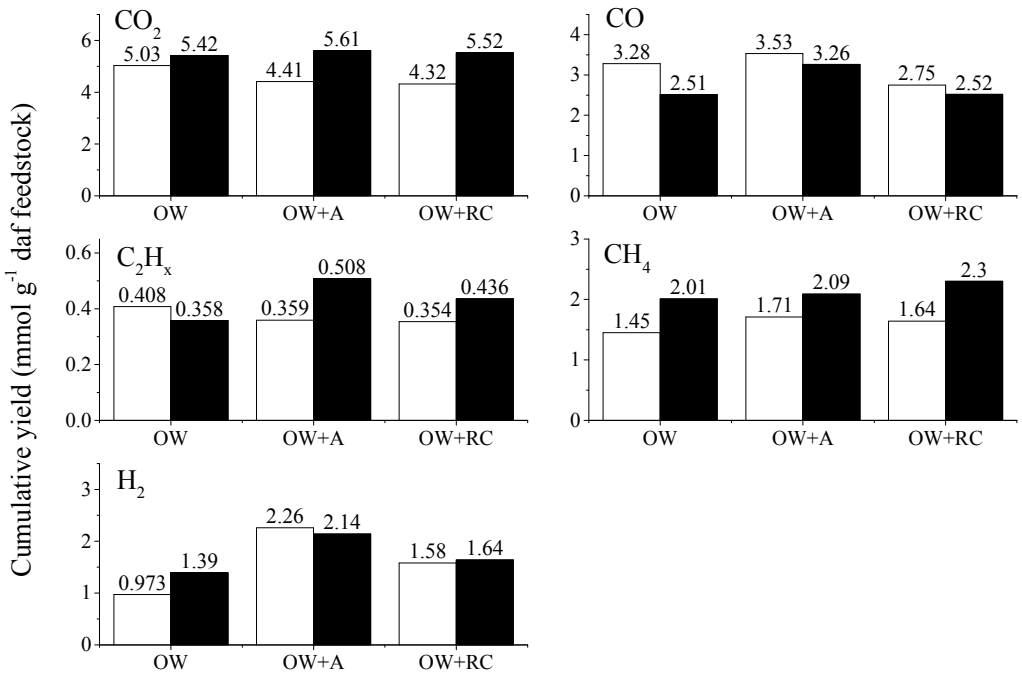

Figure 4. Cumulative yields of the main gaseous compounds (mmol g^{-1} daf feedstock). White columns correspond to pyrolysis runs at 0.1 MPa, whereas black columns refer to runs conducted at 1.0 MPa.

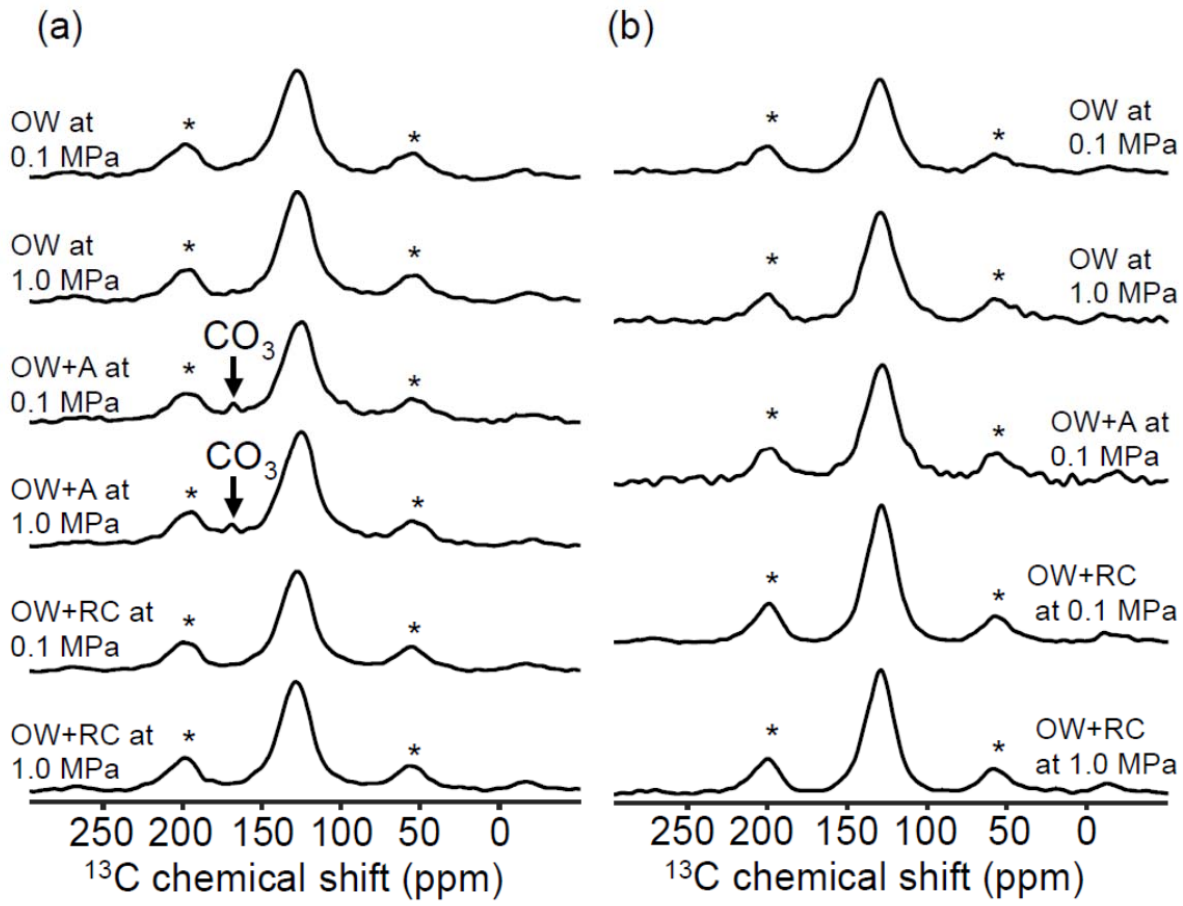

Figure 5. ^{13}C (a) DP and (b) CP NMR spectra for various samples at 7 kHz. Asterisks indicate spinning side bands.

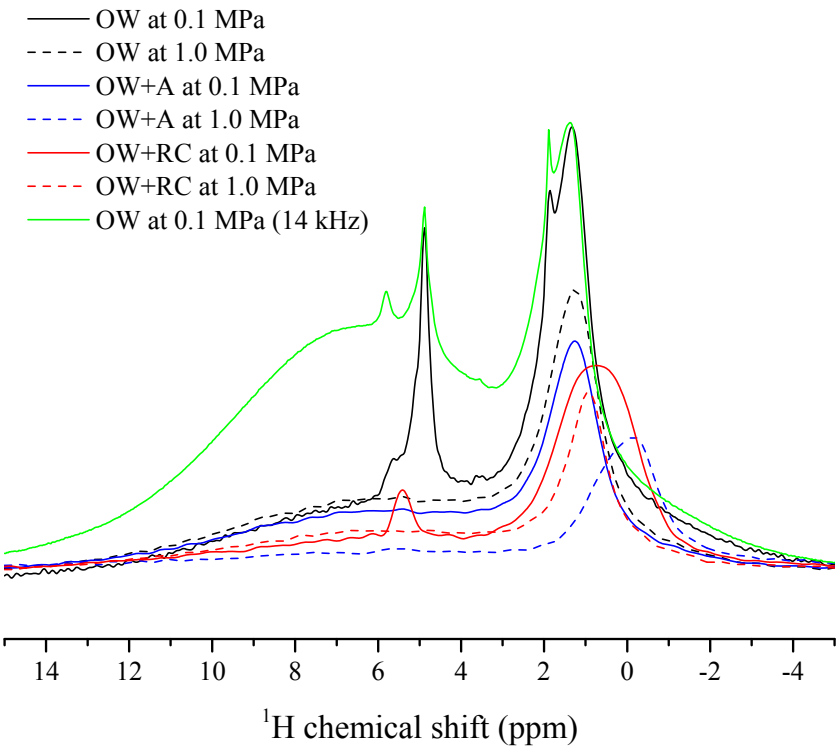

Figure 6. ^{1}H NMR spectra normalized by weight and scans. Green spectrum (OW at 0.1 MPa 14k) was acquired at 14.1 T instead of 9.4 T using a MAS frequency of 14 kHz and is not normalized. A standard baseline correction was performed.

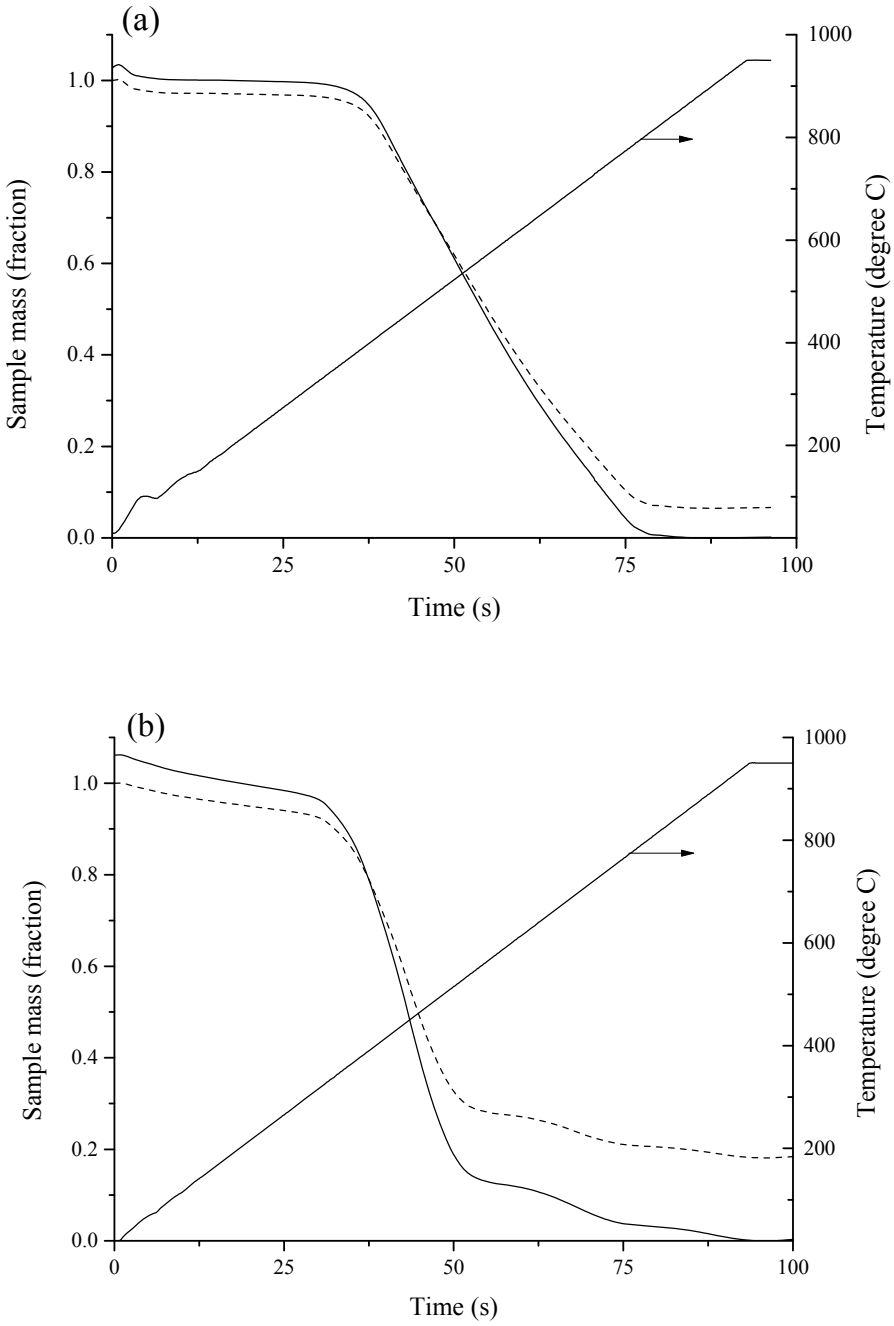

Figure 7. Uncorrected (dashed lines) and corrected (solid lines) mass-loss curves corresponding to the TPO of (a) biochar produced from OW+RC at 0.1 MPa and (b) biochar produced from OW+A at 0.1 MPa. The raw TPO data (i.e., uncorrected) were corrected for moisture and ash according to the procedure followed by Harvey et al.[12]

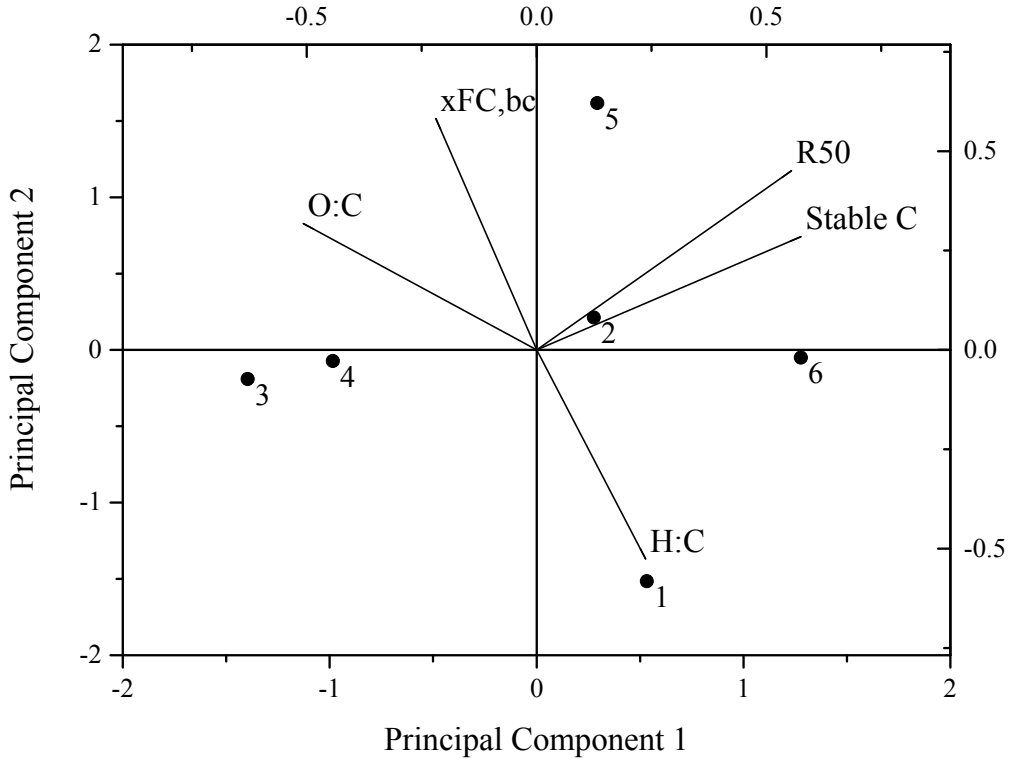

Figure 8. Bi-plot of principal components 1 and 2 derived from PCA of the correlation matrix. The first two PCs explained 71% of the variability. Labels: 1, OW at 0.1 MPa; 2, OW at 1.0 MPa; 3, OW+A at 0.1 MPa; 4, OW+A at 1.0 MPa; 5, OW+RC at 0.1 MPa; 6, OW+RC at 1.0 MPa.